Unidirectional Lasing Emerging from Frozen Light in Nonreciprocal Cavities

H. Ramezani,[1] S. Kalish,[1] I. Vitebskiy,[2] and T. Kottos[1]
[1]Department of Physics, Wesleyan University, Middletown, Connecticut 06459, USA
[2]Air Force Research Laboratory, Sensors Directorate, Wright Patterson Air Force Base, Ohio 45433, USA
(Received 21 June 2013; published 28 January 2014)

We introduce a class of unidirectional lasing modes associated with the frozen mode regime of nonreciprocal slow-wave structures. Such asymmetric modes can only exist in cavities with broken time-reversal and space inversion symmetries. Their lasing frequency coincides with a spectral stationary inflection point of the underlying passive structure and is virtually independent of its size. These unidirectional lasers can be indispensable components of photonic integrated circuitry.

DOI: 10.1103/PhysRevLett.112.043904 PACS numbers: 42.25.Bs, 42.60.Da

In the lasing process, a cavity with gain produces outgoing optical fields with a definite frequency and phase relationship, without being illuminated by coherent incoming fields at that frequency [1]. Instead, the laser is coupled to an energy source (the pump) that inverts the electron population of the gain medium, causing the onset of coherent radiation at a threshold value of the pump. In most cases the first lasing mode can be associated with a passive cavity mode. The latter is determined by the geometry and the electromagnetic constitutive parameters $\epsilon - \mu$ of the passive cavity. Above the first lasing threshold, lasers have to be treated as nonlinear systems [2], but up to the first threshold they satisfy the linear Maxwell equations with a negative imaginary part of the refractive index, generated by the population inversion due to the pump [1]. This simplification allows for a linear treatment of threshold modes within a scattering matrix formalism [3].

In this Letter, using scattering formalism, we introduce a class of unidirectional lasing modes emerging from frequencies associated to spectrally asymmetric stationary inflection points of the underlying passive photonic structure. A distinctive characteristic of these modes is that, in contrast to traditional Fabry-Perot (FP) resonances, they are virtually independent of the size and geometry of the confined photonic structure [4]. Utilizing these modes we propose to create a mirrorless unidirectional laser (MUL) which emits the outgoing optical field into a single direction. Incorporating a MUL in an optical ring resonator can result in various functionalities. Potential applications include optical ring gyroscopes in which a beat frequency between two oppositely directed unidirectional ring diode lasers is detected to measure the rotation rate, optical logic elements in which the direction of lasing in the ring is the logic state of the device, and optical signal routing elements for photonic integrated circuits where the signals are routed around a ring cavity towards a specific output coupler.

The concept of frozen modes and electromagnetic unidirectionality first emerged within the context of spectral asymmetry of nonreciprocal periodic structures [5–7]. In this regard it was recognized that magnetic photonic crystals satisfying certain symmetry conditions [7,8] can develop a strong spectral asymmetry $\Omega(\vec{k}) \neq \Omega(-\vec{k})$. An example case of such periodic arrangement is shown in Fig. 1. The basic unit consists of three components: a central magnetic layer "sandwiched" between two misaligned anisotropic layers. The magnetic layer (gray layer in Fig. 1) induces magnetic nonreciprocity which is associated with the breaking of time reversal symmetry due to a static magnetic field or spontaneous magnetization. However, breaking time-reversal symmetry is not sufficient to obtain spectral asymmetry. The symmetry analysis [7,8] shows that the absence of space inversion is also required. This is achieved with the use of two birefringent layers (blue and red layers in Fig. 1).

The constitutive tensors $\hat{\epsilon}_{1,2} - \hat{\mu}$ of the nonmagnetic layers are assumed to be

$$\hat{\boldsymbol{\epsilon}}_{1,2} = \begin{bmatrix} \epsilon_A + \delta\cos(2\phi_{1,2}) & \delta\sin(2\phi_{1,2}) & 0 \\ \delta\sin(2\phi_{1,2}) & \epsilon_A - \delta\cos(2\phi_{1,2}) & 0 \\ 0 & 0 & \epsilon_{zz} \end{bmatrix}; \quad \hat{\mu} = \hat{\mathbf{1}}, \tag{1}$$

where δ describes the magnitude of in-plane anisotropy and the angle $\phi_{1,2}$ defines the orientation of the principle

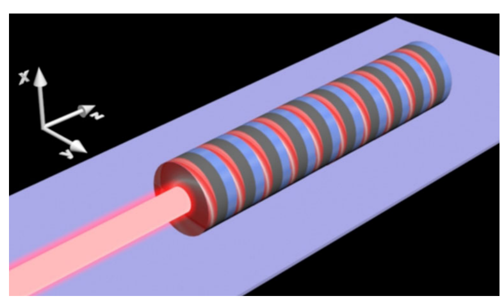

FIG. 1 (color online). Schematic of a mirrorless unidirectional laser structure. The basic unit includes three layers—a gyrotropic magnetic element layer (gray) sandwiched between two misaligned anisotropic layers (red and blue). The misalignment angle $\phi_1 - \phi_2$ must be different from 0 and $\pi/2$.

axes in the xy plane for each of the two nonmagnetic layers. The corresponding constitutive parameters for the magnetic layer are

$$\hat{\epsilon} = \begin{bmatrix} \epsilon_F & i\alpha & 0 \\ -i\alpha & \epsilon_F & 0 \\ 0 & 0 & \epsilon_{zz} \end{bmatrix}; \qquad \hat{\mu} = \begin{bmatrix} \mu_{xx} & i\beta & 0 \\ -i\beta & \mu_{xx} & 0 \\ 0 & 0 & \mu_{zz} \end{bmatrix}; \quad (2)$$

The gyrotropic parameters α, β are responsible for the magnetic Faraday rotation [9]. In the simulations below we use the same set of physical parameters as in [8]. Specifically, $\epsilon_A = 43.85$, $\delta = 42.64$, $\phi_1 = \pi/4$, $\phi_2 = 0$, $\epsilon_F = 30.525$, $\alpha = 0.625$, $\beta = 1.24317$, and $\mu_{xx} = 1.29969$. The frequency Ω is measured in units of $\Omega_0 = c/L$, i.e., $\omega \equiv \Omega/\Omega_0$, where c is the speed of light in vacuum and $L = L_A$ is the thickness of the dielectric layers. The width of the ferromagnetic layer is $L_F = 0.45L$. Without loss of generality we assume that $L = 1$.

The dispersion relation $\omega(\vec{k}) \equiv \Omega(\vec{k})/\Omega_0$ for the infinite periodic stack of Fig. 1 can be calculated numerically using a standard transfer matrix approach [8,10]. We find that $\omega(\vec{k})$ displays asymmetry with respect to the Bloch wave vector $\vec{k}$. For a given structural geometry, the degree of the spectral asymmetry depends on the magnitude of nonreciprocal circular birefringence of the magnetic layer and linear birefringence of the misaligned dielectric layers. If either of the two birefringences is too small, or too large, the spectral asymmetry becomes small. The choice of the numerical parameters allows us to clearly demonstrate the effect of unidirectional lasing using the simplest example of a periodic layered structure shown in Fig. 1. At optical frequencies, very similar results can be achieved by turning the open cavity of Fig. 1 into a ringlike structure [11].

The property of spectral asymmetry has various physical consequences, one of which is the possibility of unidirectional wave propagation [8]. Let us consider a transverse monochromatic wave propagating along the symmetry direction $\hat{z}$ of the gyrotropic photonic crystal. The Bloch wave vector $\vec{k} = k\hat{z}$, as well as the group velocity $\vec{v}(\vec{k}) \equiv \partial\omega(\vec{k})/\partial\vec{k}$ are parallel to z. In Fig. 2(a) we see that one of the spectral branches $\omega(k)$ develops a stationary inflection point (SIP) for which

$$\left.\frac{\partial\omega}{\partial k}\right|_{k=k_0} = 0; \qquad \left.\frac{\partial^2\omega}{\partial k^2}\right|_{k=k_0} = 0; \qquad \left.\frac{\partial^3\omega}{\partial k^3}\right|_{k=k_0} \neq 0. \quad (3)$$

An example of a SIP occurring at $\omega_0 \approx 5463.5$ is marked in Fig. 2(a) with a circle. At this frequency there are two propagating Bloch waves: one with $k_0 \approx 0.613$ and the other with $k_1 \approx -2.452$. Obviously, only one of the two waves can transfer electromagnetic energy—the one with $k = k_1$ and corresponding group velocity pointing in the positive $\hat{z}$ direction, i.e., $\vec{v}(k_1) > 0$. The Bloch eigenmode with $k = k_0$ has zero group velocity $\vec{v}(k_0) = 0$ and, therefore, does not transfer energy. The latter propagating mode

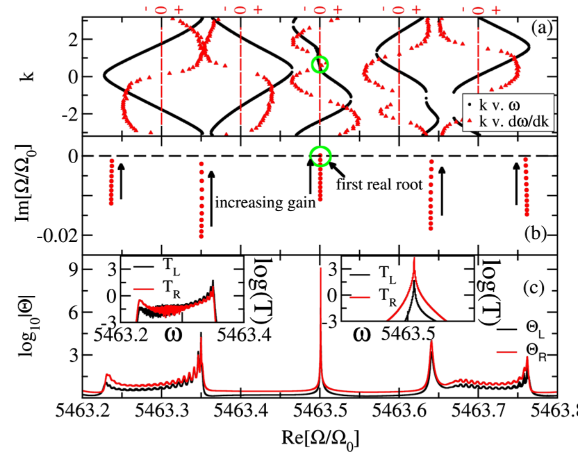

FIG. 2 (color online). (a) Asymmetric dispersion relation (black filled circles) of the rescaled frequency $\omega(k) \equiv \Omega(k)/\Omega_0$ ($\Omega_0 \equiv c/L$, where c is the speed of light and $L = L_A$ is the thickness of the dielectric layers) of the passive magnetic photonic structure shown in Fig. 1 . Overlaid is the group velocity $d\omega/dk$ of the propagating modes (red triangles). The SIP is indicated with a circle. (b) Motion of exact S-matrix poles in the complex k-plane as the gain inside the photonic structure increases from zero. The arrows indicate the direction of increasing gain. The green circle marks the first lasing threshold. (c) The response function $\Theta_{L,R}(\omega) = T_{L,R} + R_{L,R}$ vs. ω for a grating consisting of 20 basic units. Left inset: T_L left (black) and T_R right (red) transmittance for a frequency domain where Fabry-Perot resonances are present. Right inset: $T_{L,R}$ around the SIP frequency. Notice the high level of asymmetry near the SIP where $T_R \gg T_L$ (more than two order of magnitude).

is associated with a stationary inflection point Eq. (3) and referred to as the "frozen" mode. Thus a photonic crystal with the dispersion relation similar to that in Fig. 2(a) displays the property of electromagnetic unidirectionality at $\omega = \omega_0$. Such a remarkable effect is an extreme manifestation of the spectral asymmetry [8].

Next we turn to the analysis of the open structure and the emergence of unidirectional lasing modes. It can be rigorously shown within semiclassical laser theory that the first lasing mode in any cavity is an eigenvector of the electromagnetic scattering matrix (**S** matrix) with an infinite eigenvalue; i.e., lasing occurs when a pole of the **S** matrix is pulled "up" to the real axis by including gain as a negative imaginary part of the refractive index [3]. We, therefore, proceed to evaluate the scattering matrix associated with the open photonic structure of Fig. 1.

The electric $\vec{\mathbf{E}}(\vec{r})$ and magnetic $\vec{\mathbf{H}}(\vec{r})$ fields are designated by the time-harmonic Maxwell equations:

$$\nabla \times \vec{\mathbf{E}}(\vec{r}) = i\frac{\omega}{c}\hat{\mu}\vec{\mathbf{H}}(\vec{r}), \qquad \nabla \times \vec{\mathbf{H}}(\vec{r}) = -i\frac{\omega}{c}\hat{\varepsilon}\vec{\mathbf{E}}(\vec{r}) \quad (4)$$

with the solution

$$\vec{\mathbf{E}}(\vec{r}) = e^{i(k_x x + k_y y)}\vec{E}(z), \qquad \vec{\mathbf{H}}(\vec{r}) = e^{i(k_x x + k_y y)}\vec{\mathbf{H}}(z), \quad (5)$$

where $\omega(\vec{k})$ is the frequency. An "external region" encompassing the resonator, extends for $|z| > L/2$. We assume that the permittivity and permeability parameters take constant values $\hat{\boldsymbol{\epsilon}} = \epsilon_0 \times \hat{\mathbf{1}}$; $\hat{\mu} = \mu_0 \times \hat{\mathbf{1}}$ where $\hat{\mathbf{1}}$ is the 3×3 identity matrix.

Assuming normal propagation, i.e., $k_x = k_y = 0$, the solutions of Eq. (5) for $\vec{E}(z)$ in the left (l) and right (r) side of the scattering region, are written in terms of the forward and backward traveling waves:

$$\vec{E}^{l,r} = \mathbf{A}^{l,r} e^{ikz} + \mathbf{B}^{l,r} e^{-ikz}, \quad (6)$$

where

$$\mathbf{A}^{l,r} = [A_x^{l,r} \quad A_y^{l,r}]^T; \qquad \mathbf{B}^{l,r} = [B_x^{l,r} \quad B_y^{l,r}]^T. \quad (7)$$

The corresponding magnetic field $\vec{H}(z)$ is $\vec{H}(z) = \frac{1}{c}\hat{z} \times \vec{E}(z)$, where $\hat{z}$ is the unit vector in the z direction.

The relation between the electric field on the left and right sides of the scattering region is described by the 4×4 transfer matrix $\mathbf{M}$:

$$\begin{bmatrix} \mathbf{A}^r \\ \mathbf{B}^r \end{bmatrix} = \mathbf{M} \begin{bmatrix} \mathbf{A}^l \\ \mathbf{B}^l \end{bmatrix}; \qquad \mathbf{M} = \begin{bmatrix} \mathbf{M}_{11} & \mathbf{M}_{12} \\ \mathbf{M}_{21} & \mathbf{M}_{22} \end{bmatrix}. \quad (8)$$

The transmission and reflection coefficients can be then expressed in terms of the transfer matrix elements as

$$\begin{aligned} \mathbf{r}^l &= -\mathbf{M}_{22}^{-1}\mathbf{M}_{21}, \qquad \mathbf{r}^r = \mathbf{M}_{12}\mathbf{M}_{22}^{-1} \\ \mathbf{t}^l &= \mathbf{M}_{11} - \mathbf{M}_{12}\mathbf{M}_{22}{}^{-1}\mathbf{M}_{21}, \qquad \mathbf{t}^r = \mathbf{M}_{22}^{-1}. \end{aligned} \quad (9)$$

From Eqs. (9), we construct the scattering matrix $\mathbf{S}$

$$\begin{bmatrix} \mathbf{B}^l \\ \mathbf{A}^r \end{bmatrix} = \mathbf{S} \begin{bmatrix} \mathbf{A}^l \\ \mathbf{B}^r \end{bmatrix}; \qquad \mathbf{S} \equiv \begin{bmatrix} \mathbf{r}^l & \mathbf{t}^r \\ \mathbf{t}^l & \mathbf{r}^r \end{bmatrix}, \quad (10)$$

which, below the laser threshold, connects the outgoing wave amplitudes to their incoming counterparts. For lossless media the permittivity $\epsilon = \epsilon' + i\epsilon''$ is strictly real $\epsilon'' = 0$. Addition of gain in the system results in a complex permittivity $\epsilon = \epsilon' + i\epsilon''$ with $\epsilon'' < 0$. Without loss of generality we further assume that the gain is introduced at the dielectric layers with $\phi_2 = 0$. We have checked that other periodic arrangements of the gain along the cavity give the same qualitative results.

Following Refs. [3,12] we analytically continue the scattering matrix $\mathbf{S}$ to the complex-k plane. The scattering resonances are then defined by the following (outgoing) boundary conditions, i.e., $(\mathbf{B}^l, \mathbf{A}^r)^T \neq 0$ while $(\mathbf{A}^l, \mathbf{B}^r)^T = 0$, and are associated with the poles of the $\mathbf{S}$ matrix. It follows from Eqs. (9), (10) that the poles of the $\mathbf{S}$ matrix can be identified with the complex zeros of the secular equation $\det(\mathbf{M}_{22}) = 0$.

In a passive structure, where $\epsilon = \epsilon'$ is real, the complex poles of the $\mathbf{S}$ matrix $k_p = k_R - ik_I$ are located in the lower half part of the complex plane due to causality. The real part $k_R \equiv \mathcal{R}e(k_p)$ is associated with the resonant frequencies while the imaginary part $k_I \equiv \mathrm{Im}(k_p)$ describes the fact that the cavity is open [12].

In Fig. 2(b) we report the motion of the $\mathbf{S}$-matrix poles in the complex k plane. Introducing gain ϵ'' to the system leads to an (almost) vertical movement of the poles towards the real axis. This indicates that the lasing frequency $\mathrm{Re}(k_p)$ of the system is almost equal to the associated mode of the passive structure. At the critical value ϵ''_{Th} for which the first one of the poles [marked with a circle in Fig. 2(b)] crosses the real axis the system reaches the lasing threshold. We have further confirmed the lasing action at ϵ''_{Th} by evaluating in Fig. 2(c) an overall response function, defined as the total intensity of outgoing (reflected or transmitted) waves for either a left or right (single-port) injected wave; that is $\Theta_{L,R}(\omega) = T_{L,R} + R_{L,R}$, where $T_{L/R}$ and $R_{L/R}$ are the respective left and right transmittances and reflectances averaged over polarization. For a lossless passive medium, one always has $\Theta(\omega) = 1$ due to power conservation, whereas $\Theta(\omega) > 1$ indicates that an overall amplification has been realized. Near the lasing frequency $\Theta(\omega)$ takes large values, diverging as the lasing threshold is attained. Furthermore, in the insets of Fig. 2(c) we report the left and right transmittances in the regime of regular FP resonances (left inset) and at a SIP-related frozen mode (right inset). While for FP resonances T_L and T_R exhibit a moderate asymmetry, for a SIP-related mode the asymmetry between them increases dramatically ($T_R \gg T_L$ by more than 2 orders of magnitude) indicating strongly asymmetric transport.

A comparison between Fig. 2(a) and Figs. 2(b),(c) indicates that the lasing threshold frequency is very close to ω_0 associated with the SIP. While, at this frequency, a right-moving propagating wave (associated to k_1 and having large group velocity $v(k_1) > 0$) releases most of its energy outside the photonic structure, the mode associated with $k \approx k_0$ has extremely small group velocity and allows for a long residence time of the photons inside the structure. The interaction of these photons with the gain medium results in strong amplification, which in turn leads to a lasing action. Once the lasing threshold is reached, the outgoing lasing beam is emitted predominantly from the left side of our structure [opposite side from $v(k_1) > 0$], therefore producing unidirectional lasing.

We have confirmed the asymmetry in overall power amplification by analyzing the ratio $\Lambda \equiv T_R + R_L/T_L + R_R$. The latter is shown in the right column of Fig. 3. Specifically, large values of Λ indicate asymmetric power amplification towards the left while smaller than unity Λ indicates power amplification towards the right. However the actual indication of the *nonreciprocal* nature of our photonic structure is provided by an analysis of the transmittance asymmetry $T_A = T_R/T_L$. This asymmetry exists

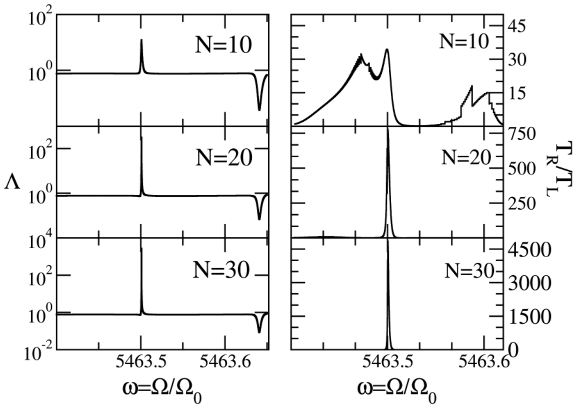

FIG. 3. The ratio Λ (left column) and the associated transmittance asymmetry $T_A = T_R/T_L$ (right column) for the photonic structure of the Fig. 1, for systems of (a) 10, (b) 20, and (c) 30 basic units. Notice that T_A increases near the SIP-related mode [while it subsides at regular FP resonances where $T_A \approx 1$, see also insets of Fig. 2(c)]. Here $\omega = \Omega/\Omega_0$ (where $\Omega_0 = c/L$) is the rescaled frequency.

only in the case that nonreciprocity and gain are simultaneously present.

The magnitude of T_A will be strongly affected by the existence of the SIP. Specifically, we expect that the unidirectional amplification near the SIP can be enhanced further by increasing the size of the periodic structure. In this case, the residence time of photons associated with the left moving (slow velocity) mode becomes even longer thus resulting in stronger transmission asymmetries. A scaling analysis of T_A for an increasing number of periods of the grating (see Fig. 3 right panels) indicates that as the system becomes larger the asymmetry becomes increasingly peaked around the unidirectional lasing mode (associated to the SIP), while other picks (associated to standard FP resonances) remain unchanged or even subside. We observe that the unidirectional lasing frequency emerging from of the SIP mode remains fixed and it is insensitive to the size of the periodic structure.

Conclusions.—We have introduced a qualitatively new mechanism for unidirectional lasing action which is independent on the dimensionality of the lasing cavity and relies on the coexistence of a nonreciprocal SIP-related frozen modes and gain. The transmittance asymmetry of these modes increases significantly with the size of the structure. As opposed to a conventional lasing cavity utilizing asymmetrically placed reflecting mirrors, a nonreciprocal magnetophotonic structure can produce unidirectionality, even at the first (linear) lasing threshold. This unique feature is not available in reciprocal active cavities. Besides, a unidirectional magnetophotonic structure does not need mirrors or any other reflectors in order to trap light and reach the lasing threshold.

The nonreciprocal layered structure in Fig. 1 is just a toy model of a periodic array capable of developing a spectral SIP. It was rather used here in order to demonstrate the proof of principle for the MUL. A future challenging research direction is to propose realistic structures that allow for the coexistence of gain and nonreciprocal SIP. While at infrared and optical wavelengths, the gain is not a problem, the creation of a well-defined nonreciprocal SIP is not a simple matter and is the subject of a whole new area of research. In this respect a promising approach that we intend to explore in the future is to replace the layered structure in Fig. 1 with an array of two or three coupled periodic optical waveguides similar to those proposed in Ref. [13]. Such arrays can support a reciprocal SIP. Our preliminary consideration shows that adding a gain component to the waveguide array and using a magnetic substrate can produce a nonreciprocal SIP, along with the necessary conditions for unidirectional lasing. Still, at this point, practical realization of a MUL remains challenging.

This work was sponsored by the Air Force Research Laboratory (AFRL/RYD) through the AMMTIAC contract with Alion Science and Technology, and by the Air Force Office of Scientific Research, Grants No. LRIR 09RY04COR and No. FA 9550-10-1-0433. Valuable comments from Dr. T. Nelson are greatly appreciated.

[1] H. Haken, *Laser Light Dynamics* (North-Holland, Amsterdam, 1986).
[2] H. E. Türeci, A. D. Stone, L. Ge, S. Rotter, and R. J. Tandy, Nonlinearity **22**, C1 (2009).
[3] K. M. Frahm, H. Schomerus, M. Patra, and C. W. J. Beenakker, Europhys. Lett. **49**, 48 (2000).
[4] A. Figotin and I. Vitebskiy, Laser Photonics Rev. **5**, 201 (2011).
[5] R. Fuchs, Philos. Mag. **11**, 647 (1965).
[6] T. O'Dell, *The Electrodynamics of Magnetoelectric Media* (North-Holland, Amsterdam, 1970).
[7] I. Vitebskiy, J. Edelkind, E. Bogachek, A. G.Scherbakov, and U. Landman, Phys. Rev. B **55**, 12 566 (1997).
[8] A. Figoton and I. Vitebsky, Phys. Rev. E **63**, 066609 (2001); Phys. Rev. B **67**, 165210 (2003).
[9] L. D. Landau, E. M. Lifshitz, and L. P. Pitaevskii, *Electrodynamics of Continous Media* (Pergamon, New York, 1984).
[10] H. Ramezani, Z. Lin, S. Kalish, T. Kottos, V. Kovanis, and I. Vitebskiy, Opt. Express **20**, 26 200 (2012).
[11] Because of the inherent weakness of Faraday rotation at optical frequencies, a SIP on the $k-\omega$ diagram will always be located in close proximity to a photonic band edge. As a consequence, the frozen mode regime in the open photonic cavity of Fig. 1 will be overwhelmed with the much more powerful and nearly perfectly symmetric, giant FP resonance [4], whose intensity scales as N^4 (N is the number of layers). A way to eliminate this and other transmission resonances and preserve the phenomenon of electromagnetic unidirectionality is to use a closed ringlike structure, instead of the open one shown in Fig. 1.

[12] L. Ge, Y. D. Chong, S. Rotter, H. E. Türeci, and A. D. Stone, Phys. Rev. A **84**, 023820 (2011).

[13] N. Gutman, W. H. Dupree, Y. Sun, A. A. Sukhorukov, and C. M. de Sterke, Opt. Express **20**, 3519 (2012); J. R. Burr, N. Gutman, C. Martijn de Sterke, I. Vitebskiy, and R. M. Reano, Opt. Express **21**, 8736 (2013); N. Gutman, C. Martijn de Sterke, A. A. Sukhorukov, and L. C. Botten, Phys. Rev. A **85**, 033804 (2012).